AGU PUBLICATIONS

JGR

Journal of Geophysical Research: Oceans

RESEARCH ARTICLE

10.1002/2015JC011583

Key Points:
- Replacement of old sea ice by first-year sea ice in the Beaufort Sea is quantified
- Delayed freeze up, not breakup timing, is responsible for lengthened summer open water duration
- Increased first-year sea ice may be affecting the formation of the Cape Bathurst flaw lead polynya

Correspondence to:
R. Galley,
ryan.galley@ad.umanitoba.ca

Citation:
Galley, R. J., D. Babb, M. Ogi, B. G. T. Else, N.-X. Geilfus, O. Crabeck, D. G. Barber, and S. Rysgaard (2016), Replacement of multiyear sea ice and changes in the open water season duration in the Beaufort Sea since 2004, *J. Geophys. Res. Oceans*, *121*, 1806–1823, doi:10.1002/2015JC011583.

Received 17 DEC 2015
Accepted 19 FEB 2016
Accepted article online 26 FEB 2016
Published online 19 MAR 2016

Replacement of multiyear sea ice and changes in the open water season duration in the Beaufort Sea since 2004

R. J. Galley[1], D. Babb[1], M. Ogi[1], B. G. T. Else[2], N.-X. Geilfus[3], O. Crabeck[1], D. G. Barber[1], and S. Rysgaard[1,3]

[1]Centre for Earth Observation Science, University of Manitoba, Winnipeg, Manitoba, Canada, [2]Department of Geography, University of Calgary, Calgary, Alberta, Canada, [3]Arctic Research Centre, Aarhus University, Aarhus, Denmark

Abstract The last decade has witnessed the nine lowest Arctic September sea ice extents in the observational record. It also forms the most recent third of the long-term trend in that record, which reached −13.4% decade^{-1} in 2015. While hemispheric analyses paint a compelling picture of sea ice loss across the Arctic, the situation with multiyear ice in the Beaufort Sea is particularly dire. This study was undertaken in light of substantial changes that have occurred in the extent of summer multiyear sea ice in the Arctic inferred from the passive microwave record. To better elucidate these changes at a sub-regional scale, we use data from the Canadian Ice Service archive, the most direct observations of sea ice stage-of-development available. We also build upon the only previous sea ice climatological analysis for Canada's western Arctic region by sea ice stage-of-development that ended in 2004. The annual evolution of sea ice by stage of development in Canada's western Arctic changed dramatically between 1983 and 2014. The rate of these changes and their spatial prevalence were most prominent in the last decade. In summer, total sea ice loss occurred via reductions in old and first-year sea ice over increasingly large areas and over more months per year. Resultant delay of thermodynamic freeze up has increased the annual open water duration in the study region. The winter sea ice cover was increasingly composed of first-year sea ice at the expense of old ice. Breakup timing has not significantly changed in the region.

1. Introduction

Between 1979 and 2015, mean September Arctic sea ice extent decreased by 13.4% decade^{-1}, a trend that has nearly doubled in magnitude since 2001 [*Fetterer et al*., 2002]. Within the long-term time series, nine of the lowest sea ice extents in the observational record occurred between 2007 and 2015 [*Fetterer et al*., 2002]. Declining sea ice extent coupled with pan-Arctic trends toward younger [*Ngheim et al*., 2006; *Maslanik et al*., 2007, 2011], thinner [*Kwok and Rothrock*, 2009; *Kwok et al*., 2009] sea ice have reduced the Arctic sea ice volume [*Kwok et al*., 2009; *Zhang et al*., 2012].

Analyses of the passive microwave (PM) sea ice concentration data from the U.S. National Snow and Ice Data Center (NSIDC) indicate that for a 30 year period ending in 2008 and a 35 year period ending in 2013, the sea ice extent (the area covered by a minimum 15% concentration) season got shorter almost everywhere in the Arctic [*Parkinson*, 2014]. Changes in the Arctic sea ice melt season length computed using the NSIDC PM sea ice concentration record [*Stroeve et al*., 2014] indicate that trends therein correspond generally with the sea ice season length trends for the same period; i.e., where positive trends in the melt season length occurred, negative trends in the sea ice season length were generally observed.

Recently decreased summer sea ice extents have been in part created by reduced sea ice concentrations in the Arctic's peripheral seas, which has intensified in particular in the East Siberian, Chukchi and Beaufort Seas. The melt season length between 1979 and 2013 in the peripheral seas of the Arctic Ocean (Beaufort, Chukchi, East Siberian, Kara, and Laptev Seas) was 3–5 months on average in the PM data, though interannual variability was high [*Stroeve et al*., 2014]. *Parkinson* [2014] determined the trend in the length of the sea ice season in the Canada Basin of the Arctic Ocean was −10 to −30 days·decade^{-1} as part of a larger hemispheric analysis. Trends (1979–2013) in the melt season length derived from the NSIDC PM sea ice concentration data in the Beaufort Sea were about 9 days·decade^{-1}, composed of statistically significant

(>95% level) trends toward earlier melt onset (−2.5 days·decade^{-1}) and later freeze up (6.5 days·decade^{-1}) [*Stroeve et al*., 2014].

While these hemispheric and basin-scale analyses paint a compelling picture of sea ice loss across the Arctic, the situation for certain ice types in certain subregions––like multiyear ice in the Beaufort Sea––is particularly dire. Using passive microwave imagery and ice drift modeling, the estimated mean survival (defined as the difference between extent in mid May and at the September minimum) of multiyear sea ice extent in the Beaufort Sea decreased from 93% over the period 1981–2005 to 73% between 2006 and 2010, with multiyear sea ice largely confined to the eastern edge of the region [*Maslanik et al*., 2011]. Following earlier work that called for research into changes in concentration and trends within the Arctic's multiyear sea ice cover [*Maslanik et al*., 2007], *Maslanik et al*. [2011] concluded that a "basic shift" occurred in the late 2000s where the Canada Basin accounted for a large portion of the multiyear sea ice extent loss within the Arctic Ocean. Their PM data set from 1980 to summer 2010 suggested almost all of the observed multiyear sea ice extent loss was due to melt (as opposed to dynamic export) because: (i) of the relatively short annual period (May–September) during which the multiyear loss was observed, and (ii) the direction of sea ice motion [*Maslanik et al*., 2011]. On the other hand, *Hutchings and Rigor* [2012] revealed in great detail the dynamic processes in part responsible for anomalous summer sea ice extents in the Beaufort Sea region using NSIDC PM sea ice concentration data between 1979 and 2007. Atmospheric forcing of Arctic sea ice concentrations, especially in summer, has also been the focus of *Deser and Teng* [2008], *Ogi and Yamazaki* [2010], and *Ogi and Rigor* [2013] among others. Studies on key aspects of sea ice loss in the Beaufort Sea would likely benefit from data that provides direct observation of sea ice age.

Along with ongoing sea ice losses, the Beaufort Sea is also interesting in terms of its role in the physical evolution of multiyear sea ice [e.g., *Perovich et al*., 2008; *Haas et al*., 2010], its importance to regional biology [*Carmack and Macdonald*, 2002] and biogeochemistry [*Else et al*., 2012], and its potential for future offshore oil development [*Galley et al*., 2013]. Previous studies of sea ice in the Beaufort Sea indicate the presence of the Cape Bathurst flaw lead polynya complex [*Hammill*, 1987; *Barber and Hanesiak*, 2004; *Barber and Massom*, 2007; *Galley et al*., 2008], which operates at the interface of the predominately seasonal and multiyear sea ice regimes in the region. Sea ice within the flaw lead complex of the southern Beaufort Sea region plays an integral role in the creation of a physically favorable environment for biological production in the area [*Carmack and Macdonald*, 2002; *Arrigo and van Dijken*, 2004]. In the past, the Beaufort Gyre has played a key role in forming multiyear ice that is later exported to other regions of the Arctic. This makes increased multiyear ice melt within the Beaufort Sea significant; between 2005 and 2008 it accounted for approximately one-third of the pan-Arctic reduction in multiyear ice [*Kwok and Cunningham*, 2010]. If multiyear ice is no longer able to survive the southern pass of the Beaufort Gyre through the Beaufort Sea, the clockwise journey of multiyear ice may cease [*Maslanik et al*., 2007] and have consequences downstream of the Beaufort. Specifically, younger ice will be recirculated within the Beaufort Gyre [*Hutchings and Rigor*, 2012] and transported into the Transpolar Drift Stream [*Haas*, 2004], which has implications for the type and thickness of sea ice exported through Fram Strait [e.g., *Hansen et al*., 2013] or transported back into the Beaufort Sea. A subregional analysis focusing on the southeastern Beaufort Sea is therefore vital; increasingly studies are finding that processes with hemispheric effects occur at local or regional scales [e.g., *Kwok and Cunningham*, 2010].

This study was undertaken in light of substantial changes which have occurred in the extent of summer multiyear sea ice in the Arctic inferred from the passive microwave record [*Maslanik et al*., 2007, 2011; *Comiso*, 2012] and observational evidence of changes in the sea ice of the Beaufort Sea since 2007 [*Perovich et al*., 2008; *Kwok et al*., 2009; *Haas et al*., 2010; *Kwok and Cunningham*, 2010; *Perovich et al*., 2011; *Galley et al*., 2013]. To better elucidate these changes at a sub-regional scale, we use data from the Canadian Ice Service archive, the most direct observations of sea ice stage-of-development available. Our goal is to provide an alternative look at multiyear ice in the Beaufort Sea, addressing some of the uncertainties from less direct passive microwave and drift modeling observations. We also build upon the only previous sea ice climatological analysis for Canada's western Arctic region by sea ice stage-of-development that ended in 2004 [*Galley et al*., 2008], prior to many dramatic changes in the region. We quantify sea ice concentrations by stage-of-development in the southern Beaufort Sea, M'Clure Strait and Amundsen Gulf and temporal trends therein for a 32 year period ending in 2014. These results are compared to the same analysis ending in 2004 to accurately determine the rate at which sea ice, subdivided for new-plus-young sea ice (<30 cm),

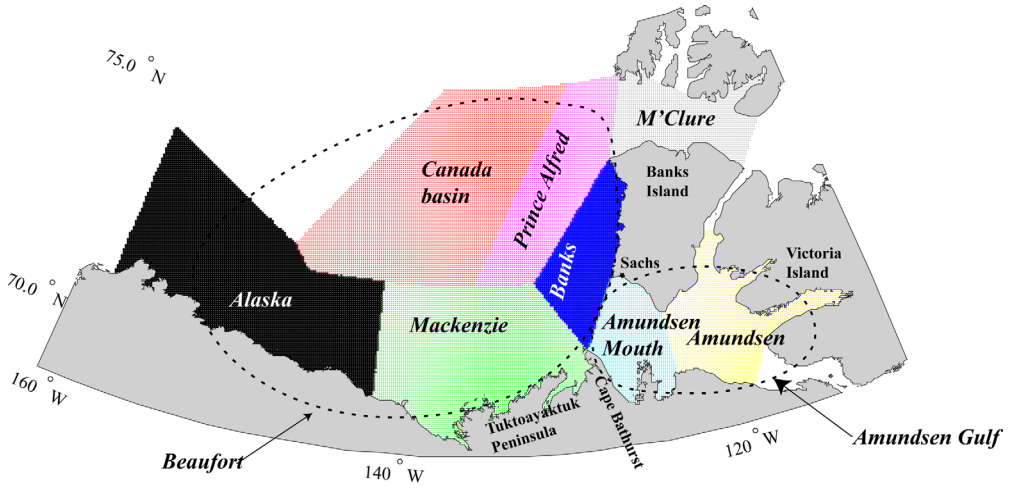

Figure 1. Map of the study area, including the locations of the Canadian Ice Service ice regime sub-regions in Canada's western Arctic region. *Amundsen Gulf* is a superset of subregions Amundsen and Amundsen Mouth, and *Beaufort* is a superset of the Alaska, Mackenzie, Canada Basin, Prince Alfred, and Banks subregions.

first-year sea ice, and old sea ice is lost, and the rate by which old sea ice is being replaced by first-year sea ice seasonally for summer and winter, and throughout the annual cycle. This work reveals the effect of the last 10 years (2005–2014) on the long-term means and trends of total sea ice and each of its contributing stages of development (i.e., new-plus-young ice, first-year sea ice and old sea ice) over the annual cycle using a data set largely based on manually classified RADARSAT images. Mean open water duration and trends in open water duration for the two time series (1983–2014 (32 years) and 1983–2004 (22 years)), are described using average breakup and freeze up dates in the region and its subregions.

2. Methods and Data

The Canadian Ice Service digital archive data set for the western Arctic region is employed in this study (CISDA, freely available at http://iceweb1.cis.ec.gc.ca/Archive/?lang=en). The CISDA is a unique and reliable data set that reports ice conditions on a weekly basis by expert manual definition of polygons from remotely sensed imagery (principally synthetic aperture RADAR since 1996) and ship- and air-borne observations using the World Meteorological Organization's egg code, which contains information on the total ice concentration (/10ths) and partial (subsets of the total) concentrations of up to three predominant stages of development (/10ths) [*Fequet*, 2005]. An extensive explanation of the suitability of these data for climatological and trend analyses is contained in *Tivy et al*. [2011].

Agnew and Howell [2003] indicate considerable discrepancy between the CISDA and NSIDC passive microwave sea ice concentration data [*Cavalieri et al*., 1996], which they attribute to tie points in the NASA Team algorithm (i) performing better at the hemispheric rather than regional scale, (ii) performing poorly in seasonal ice zone areas throughout the annual cycle, and (iii) performing poorly during melt and freeze up conditions (with greatest underestimation during the melt season), consistently underestimating the total sea ice extent. So it follows specifically that analyses undertaken regionally, in seasonal ice zones, on freeze up and melt/break up seasons might best employ these CISDA data, or perhaps the National Ice Center (NIC) archive which includes stage of development from 1995 to 2007 if an Arctic-wide product is needed [*National Ice Center*, 2009].

Each available digital ice chart for the western Arctic region was gridded from its native ArcInfo interchange format (.e00) to a 2 km × 2 km grid on a Lambert Conformal Conic projection by first converting the .e00 files to shapefiles in ArcView and then gridding them using the mapping toolbox in MATLAB. The ($4km^2$) grid cell size employed is small enough to appropriately delineate polygonal ice information and coastlines, and large enough to enable rapid computation over large areas and time scales. The area-of-interest (Figure 1) encompassed 127,734 grid cells covering 510,936 km^2 of ocean surface. The CISDA composed two time series analyzed here: the first from 1983 to 2004 (inclusive, 22 years) is composed of 800 individual charts; the second from 1983 to 2014 (inclusive, 32 years) is composed of 1260 charts.

Ice regime regions and subregions thereof, predefined by the Canadian Ice Service (CIS) (Figure 1), are employed in order to show trends in sea ice concentration by stage of development at a monthly time step in both the 22 year and 32 year time series. CIS ice regime (sub)regions represent areas for which time series can be constructed, defined in consultation with operational and research sea ice experts in conjunction with review of many existing schemes developed to meet the needs of a wide variety of research and operational stakeholders [*CIS*, 2007]. The CIS *Beaufort* ice regime region is composed of five ice regime subregions, namely *Alaska*, *Mackenzie*, *Banks*, *Prince Alfred*, and *Canada basin* (Figure 1). The *Canada basin* subregion (Figure 1) should not be confused with the much larger Canada Basin proper of the Arctic Ocean interrogated by *Parkinson* [2014]. The monthly trends in total, old, first year, and new-plus-young sea ice stages of development were also analyzed for the CIS ice regime subregions *M'Clure*, *Amundsen Mouth*, and *Amundsen*, the latter two of which have additionally been analyzed as a superset called *Amundsen Gulf* (Figure 1). We include *M'Clure*, *Amundsen*, and *Amundsen Mouth* in the monthly analysis of our study region after *Kwok and Cunningham* [2010]. December was not included in the monthly linear trend analysis because there were too few CISDA ice charts in December (as a result of a dearth of ice operations in that month) since 1983 to construct meaningful time series for that month.

The summer (July, August, September (JAS)) mean total ice, old ice (a superset of second-year and multiyear sea ice), and first-year sea ice concentrations for 1983–2004 and 1983–2014 were calculated. Subtracting the 1983–2004 means from the 1983–2014 means created differences in the three stages of development to illustrate the effect of the last 10 years on the time series. Multiple years of anomalous sea ice conditions were observed in the Beaufort Sea after 2005 [e.g., *Stroeve et al*., 2008; *Hutchings and Rigor*, 2012] and the previous analysis for the region [*Galley et al*., 2008] ended in 2004. Negative mean difference values indicate a loss of sea ice by stage of development in the 1983–2014 period relative to the 1983–2004 period. Trends in those concentrations in summer (JAS) over time for both the 1983–2004 and 1983–2014 periods were calculated using least squares fit regression. The same analyses (mean, difference, and trends) were completed for the winter (January, February, March (JFM)) sea ice concentrations, with the addition of the seasonally pertinent new-plus-young sea ice ($<$30 cm thickness) stage of development (see e.g., Figures 2 and 3).

The start and end of breakup in each grid cell are defined as the year-week that total sea ice concentration fell below eight and two tenths, respectively. Conversely the start and end of freeze up are defined as the year-week that total sea ice concentration surpassed two and eight tenths, respectively. Two tenths was used as the minimum threshold because extent is defined by 15% concentration making two-tenths the closest approximation of sea ice extent given the (semi) ordinal concentration data in the CISDA. Two and eight tenths thresholds also facilitate comparison with earlier works in the region [e.g., *Hammill*, 1987; *Galley et al*., 2008]. *Parkinson* [2014] analyzed multiple thresholds and note that the chosen threshold did not affect computation of length of sea ice season trends. The percent occurrence (i.e., the number of times the threshold was reached in the number of years analyzed) of breakup start and end were calculated for each cell, with contours of 99%, 75% and 50% overlaid on the figures. Trends in the start and end of breakup and freeze up dates, along with the annual open water duration for both time periods were computed for each grid cell where the occurrence of each of these values was $>$50%. The open water duration in each year was given by the number of weeks between the end of break up and the start of freeze up. Trends in the start and end of breakup and freeze up dates, and for the annual open water duration were computed using least squares fit regression for the 1983–2004 and 1983–2014 periods. The significance of each linear trend computed in this work was tested using a standard F-test [*Moore*, 1995]. The trend data were tested for normality and autocorrelation, which were low enough for parametric analysis. Any trend with an associated p-value less than 0.10 (different from chance at $>$ 90% level) is considered statistically significant in this work.

3. Results

3.1. Winter (JFM) Mean Concentration, Difference and Trends

Between 1983–2004 and 1983–2014 there was no considerable change in the mean total winter sea ice concentration in the western Arctic, but the addition of the last 10 years (2005–2014) to the data set reveals substantial changes in the contributions of old ice, first-year ice and young-plus-new ice (Figure 2). The

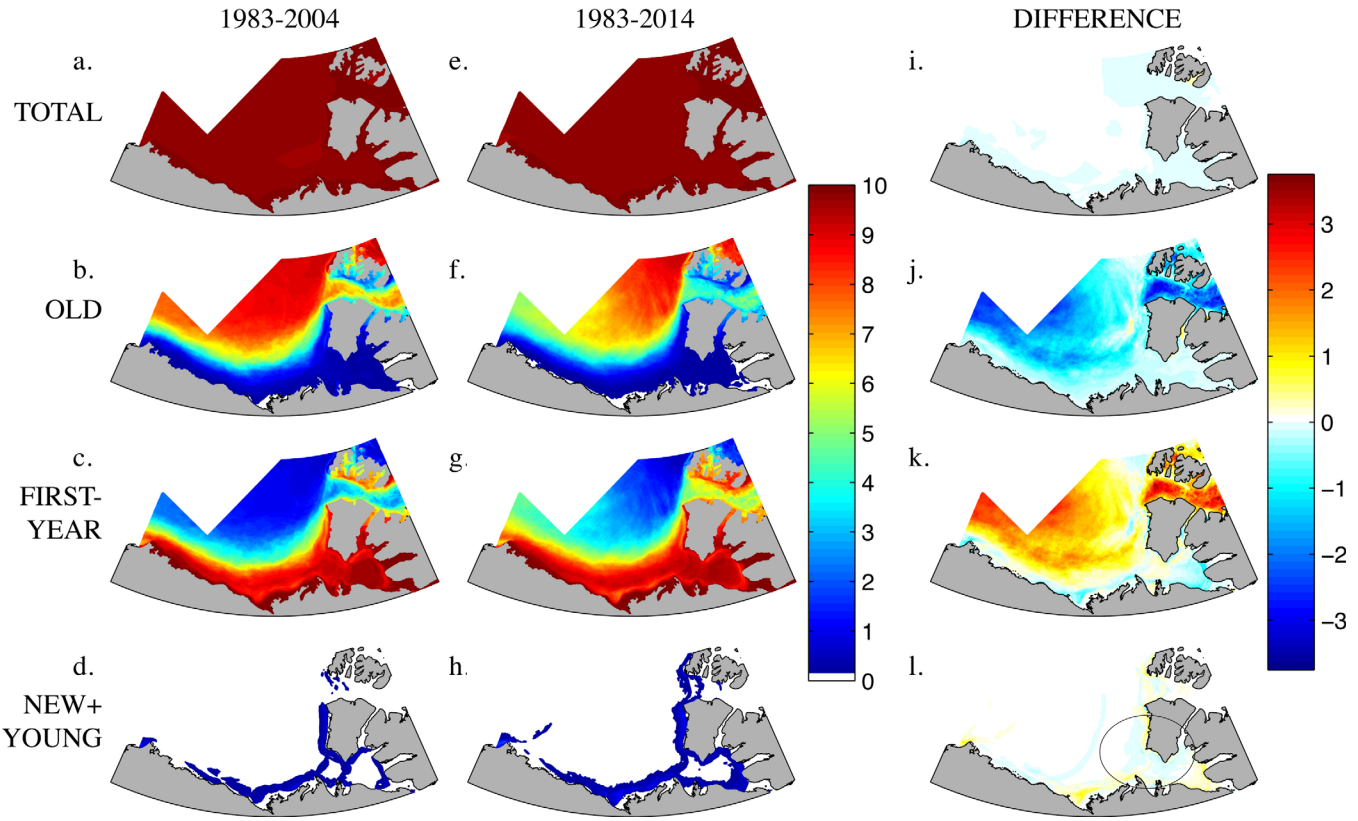

Figure 2. Mean winter (JFM) sea ice concentration (tenths) by stage of development: (a, e) total, (b, f) old ice, (c, g) first-year, and (d, h) new-plus-young ice for the 1983–2004 (left column) and the 1983–2014 periods (middle column). The difference between the two periods is shown in (right column) (i) total, (j) old, (k) first-year, and (l) new-plus-young sea ice where negative difference values indicate a reduction in the concentration since 2004.

mean winter old ice concentration for 1983–2014 compared to the 1983–2004 period decreased by more than three tenths in much of M'Clure Strait, and by 1–3 tenths in much of the Beaufort Sea (Figure 2). Conversely, the mean winter first year ice over 1983–2014 increased markedly in M'Clure Strait (>3 tenths) and in the Beaufort Sea (1–3 tenths), leaving little or no change in the winter total mean sea ice concentration in these areas but substantially reducing the winter sea ice volume. Finally, the addition of 2005–2014 to the analysis decreased the mean winter new-plus-young sea ice type (that is, the presence of persistent leads or polynyas in the winter as part of the Cape Bathurst flaw lead polynya complex, best illustrated by the presence of new and young sea ice in winter (Figure 2h)) west of Banks Island and in Amundsen Gulf (Figure 2). Although the change in new-plus-young sea ice concentration between the two periods is small, it marks a substantial decrease in the relative amount of this stage-of-development as the new-plus-young sea ice mean for 1983–2004 was <3 tenths (Figure 2l, circled in black).

Trends in the mean winter sea ice concentrations by stage-of-development indicate the region lost total sea ice at the same rate in the same areas in both the 1983–2004 and 1983–2014 periods (Figure 3). However, trends toward reduced old sea ice and increased first-year sea ice concentrations in the 1983–2004 period have been increased in magnitude by the addition of 2005–2014 to the analyses. In the 22 year period, replacement of old sea ice by first-year sea ice was limited to the edge of the winter old ice pack, and within the flaw leads north of the continental coast and west of Banks Island (Figure 3). The 1983–2014 time series reveals widespread reductions in old ice concentrations in areas in the Beaufort Sea and M'Clure Strait previously dominated by old ice in winter. Positive trends in winter first-year sea ice concentrations occur where winter reductions in old ice are observed (Figure 3). Increasingly negative trends in old sea ice concentration are observed over a larger portion of the study area between the two periods. Old ice loss has been taken up by increasingly positive trends in first-year sea ice concentrations over a larger area between 1983 and 2014, and decreasing trends in new-plus-young sea ice exist in both time series in winter (Figure 3).

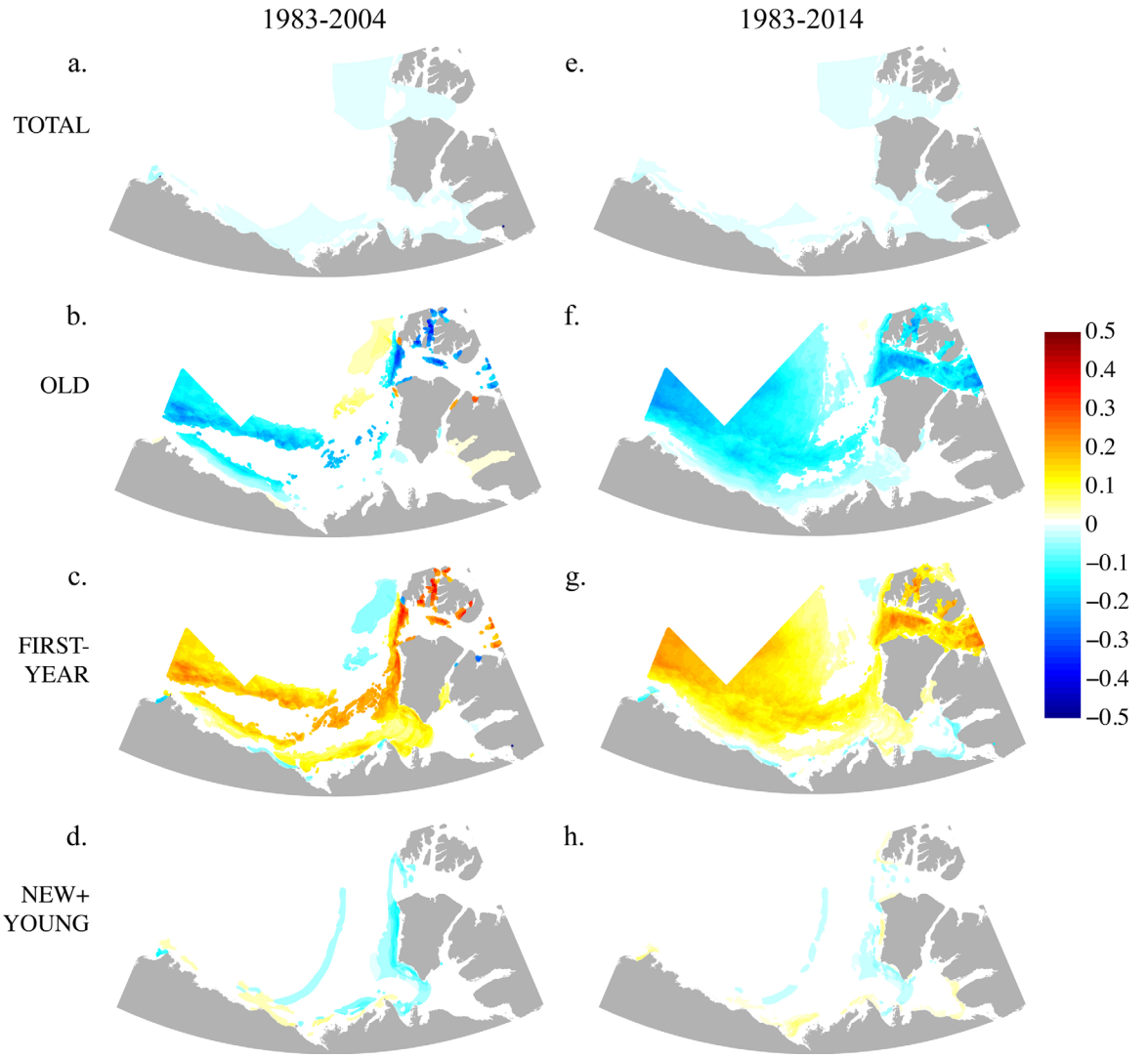

Figure 3. Trends (tenths yr^{-1}) in mean winter (JFM) sea ice concentration by stage of development; (a, e) total, (b, f) old, (c, g) first-year, and (d, h) young, for 1983–2004 (left column) and 1983–2014 (right column). Trend data only presented where $p < 0.10$.

3.2. Summer (JAS) Mean Concentration, Difference and Trends

During summer there was a considerable decrease in total sea ice concentration throughout the entire western Arctic region driven by reductions in old and first-year sea ice concentrations (Figure 4). Total sea ice losses of up to −2 tenths occurred in the transition zone at the summer sea ice pack edge where the mean sea ice concentrations increase rapidly from south to north and from Banks Island westward into the Beaufort Sea (Figure 4). Loss of summer mean total sea ice is in part caused by reduction of the mean summer old ice in the Canada basin, Banks and M'Clure (sub)regions, and a reduction of first-year sea ice, especially in the Alaska subregion (Figure 4). Reduction of mean summer old sea ice (1983–2014) is only in part compensated for by increased first-year sea ice concentrations in the eastern side of the Canada basin and the M'Clure Strait subregions (Figure 4).

Summer total, old and first-year sea ice mean concentration trends indicate the rate and spatial extent of total sea ice loss have increased dramatically in summer in the 1983–2014 period compared to 1983–2004 (Figure 5). The rate of total sea ice loss is most extreme in the southwest portion of the study area in both the 22 and 32 year periods, but nearly the entire study area experienced a negative trend in total sea ice concentration between 1983 and 2014 (Figure 5). Negative trends in mean summer total sea ice are composed of negative trends in both old and first-year sea ice concentrations, however old and first-year sea ice experienced negative trends in separate parts of the study region where their largest mean summer

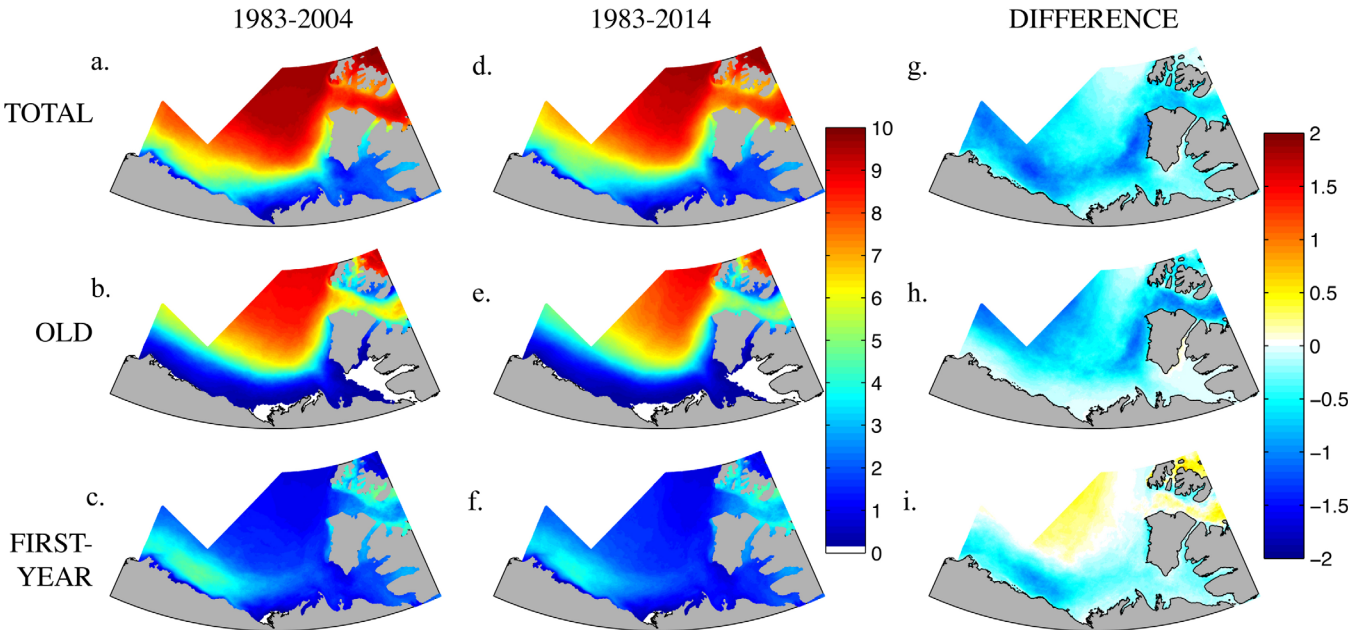

Figure 4. Mean summer (JAS) sea ice concentration (tenths) by stage of development; (a, d) total, (b, e) old and (c, f) first-year for 1983–2004 (left column) and 1983–2014 (middle column). (g, h, i) The right column indicates the difference between the two periods for the three stages of development where negative values indicate a reduction in the concentration (tenths) by stage of development in the 1983–2014 period (i.e., a loss of ice since 2004).

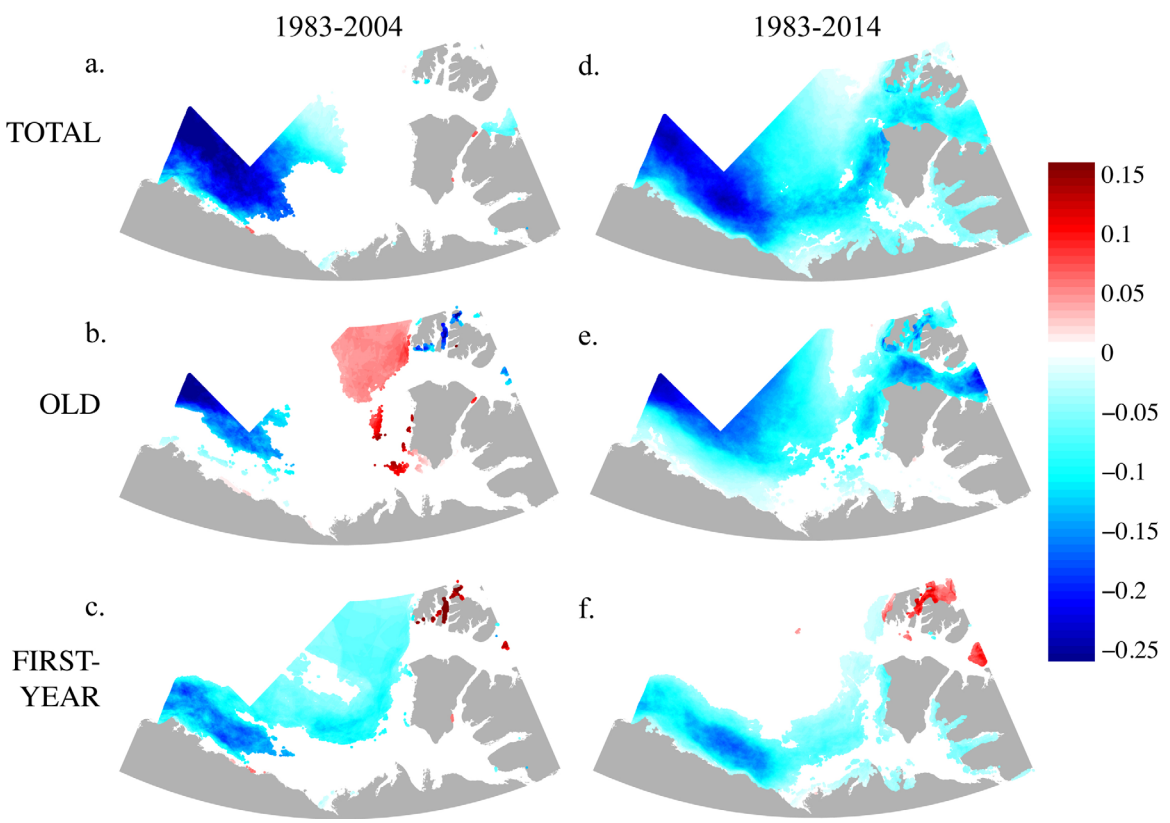

Figure 5. Trends (tenths yr^{-1}) in mean summer (JAS) sea ice concentration by stage of development; (a, d) total, (b, e) old, and (c, f) first-year, for 1983–2004 and 1983–2014. Trend data only presented where $p < 0.10$.

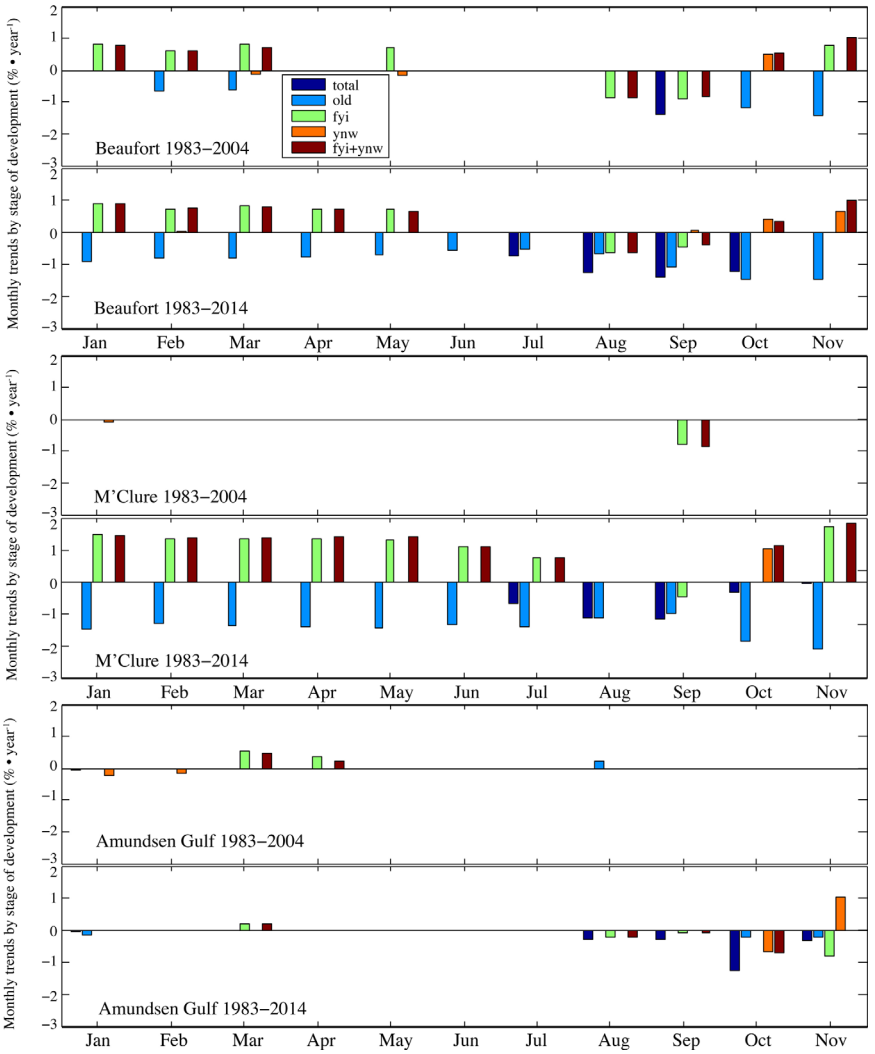

Figure 6. Trends (% yr^{-1}) in monthly mean sea ice concentration by stage of development in the Beaufort, M'Clure, and Amundsen Gulf regions from 1983 to 2004 and from 1983 to 2014. Trend data only presented where $p < 0.10$.

concentrations occurred (Figure 4). The Canada basin, Prince Alfred and M'Clure subregions experienced large negative trends in old sea ice concentrations between 1983 and 2014. The periphery of the summer sea ice pack in the study area (Alaska, Mackenzie, Banks) experienced large negative trends in first-year sea ice concentrations between 1983 and 2014. All these negative trends increased in magnitude by the addition of 2005–2014 to the time series (Figure 5).

3.3. Monthly Trends by Region/Subregion

Monthly trend analyses of total, old, first-year and young-plus-new sea ice concentrations in the Beaufort, M'Clure, and Amundsen Gulf regions further illuminate the temporal nature of changes in the sea ice cover over the annual cycle (Figure 6). In the Beaufort region between 1983 and 2004, only September experienced a negative trend in total sea ice concentration, however with the addition of the last decade, negative trends in total sea ice concentration occurred in July, August, September, and October between 1983 and 2014 (Figure 6). Between 1983 and 2014, negative trends in old sea ice concentration in the Beaufort region occurred in all eleven months analyzed compared to a few months of old ice loss in the 22 year period (Figure 6). Declining old ice concentrations in the Beaufort region between 1983 and 2014 were partly opposed by smaller positive trends in first-year sea ice from January to May, and were opposed by smaller positive trends in new-plus-young sea ice in October and November, indicating that the proportion of old and first-year stages of development in the region has changed substantially between 1983 and 2014

for the autumn, winter and spring; both the magnitude and significance of all these trends has increased since the previous period (1983–2004) in the Beaufort region (Figure 6).

Between 1983 and 2004 in the M'Clure region, almost no changes in sea ice concentration occurred, but the 1983–2014 time series reveals massive differences in the sea ice of M'Clure Strait as a result of the addition of 2005–2014 to the time series (Figure 6). Statistically significant losses in total sea ice occurred in July, August, September and October between 1983 and 2014. Negative trends in old sea ice also occur in July, August, September and October, with a positive first-year sea ice trend partially compensating for the old ice reduction in July, a positive new-plus-young sea ice trend partially counterbalancing the old ice reduction in October, and a negative first-year sea ice trend abetting the old ice reduction in September (Figure 6). Although January through June and November did not show trends in total sea ice concentration, large negative trends in old ice concentration occurred monthly in M'Clure Strait between 1983 and 2014 offset by approximately equal positive trends in first-year sea ice concentrations (Figure 6). In the M'Clure Strait subregion, the old sea ice concentration is now significantly decreased year round. Outside of the July–October melt season it is being replaced by first-year sea ice.

Although Amundsen Gulf and M'Clure Strait are similar entrances to the Canadian Arctic Archipelago separated by $<$ 300 km, their respective sea ice covers have undergone very different changes. Between 1983 and 2004 in Amundsen Gulf, only small declining trends in young-plus-new sea ice concentration in January and February, and a trend toward smaller first-year sea ice concentration in September and increasing trends in first-year sea ice concentration in March and April were found (Figure 6). With the addition of 2005–2014 to the time series, negative trends in total sea ice concentration were revealed in August, September, October and November between 1983 and 2014 (Figure 6). In August and September, negative trends in first-year sea ice concentration contributed to total ice loss in those months, whereas total ice loss in October was caused by a negative trend in new-plus-young sea ice. First-year sea ice concentration losses and new-plus-young concentrations gains offset each other leading to small negative total ice concentration trend in November (Figure 6). There is less sea ice in Amundsen Gulf now in the summer and fall, and sea ice is forming later in November instead of October.

The Beaufort region (Figures 1) is quite large, and significant and substantial disparate spatial trends in summer and winter sea ice concentrations occurred in the region (Figures 2 and 4) so monthly analysis was conducted on its five Canadian Ice Service Ice Regime subregions (Figure 7). Results indicate the addition of 2005–2014 to the time series increased prevalence of statistically significant trends in sea ice concentration in the Beaufort and reveal marked spatial variability of monthly sea ice concentration trends by stage-of-development (Figure 7).

Between 1983 and 2014, total and old sea ice losses in summer and fall months yield substantial and significant decreasing trends in old ice concentrations and increasing trends in first-year sea ice between January and June (Figure 7). Positive trends in new-plus-young sea ice concentrations occur in the 1983–2014 time series in October and/or November in each of the five Beaufort subregions (Figure 7), indicating that freeze up and related sea ice thickening occurs later and has proceeded more slowly over the long term, or that there is more open water at the end of summer which then experiences sea ice formation in autumn. In the 32 year time series, negative trends in total sea ice concentration occurred in more summer months of the year in more of the subregions of the Beaufort Sea, which temporally evolve into increasing trends in new-plus-young and first-year ice concentrations in autumn (Figure 7). As the Beaufort Sea progresses annually into winter, what follows are increasing trends in first-year sea ice combined with the nearly equal and opposite decreasing trends in old ice concentrations throughout the winter and spring months in especially the south and west subregions (Alaska, Mackenzie and Canada basin) (Figure 7). This subregional assessment agrees with the calculated summer (Figure 4) and winter (Figure 2) average sea ice concentration differences spatially and temporally.

3.4. Sea Ice Breakup

Breakup begins around year-week 20 ($\sim$15 May) in the Cape Bathurst flaw lead polynya complex of the Beaufort Sea region (Figure 8), in the areas where new and young sea ice persists in the winter historically (e.g., Figures 2d and 2h). Break up occurs next in the Amundsen and M'Clure subregions about year-week 25 (mid-June) followed by the near shore landfast sea ice areas along the continental coast and in embayments surrounding Amundsen Gulf [e.g. *Galley et al.*, 2012]. Landfast areas begin to breakup about the

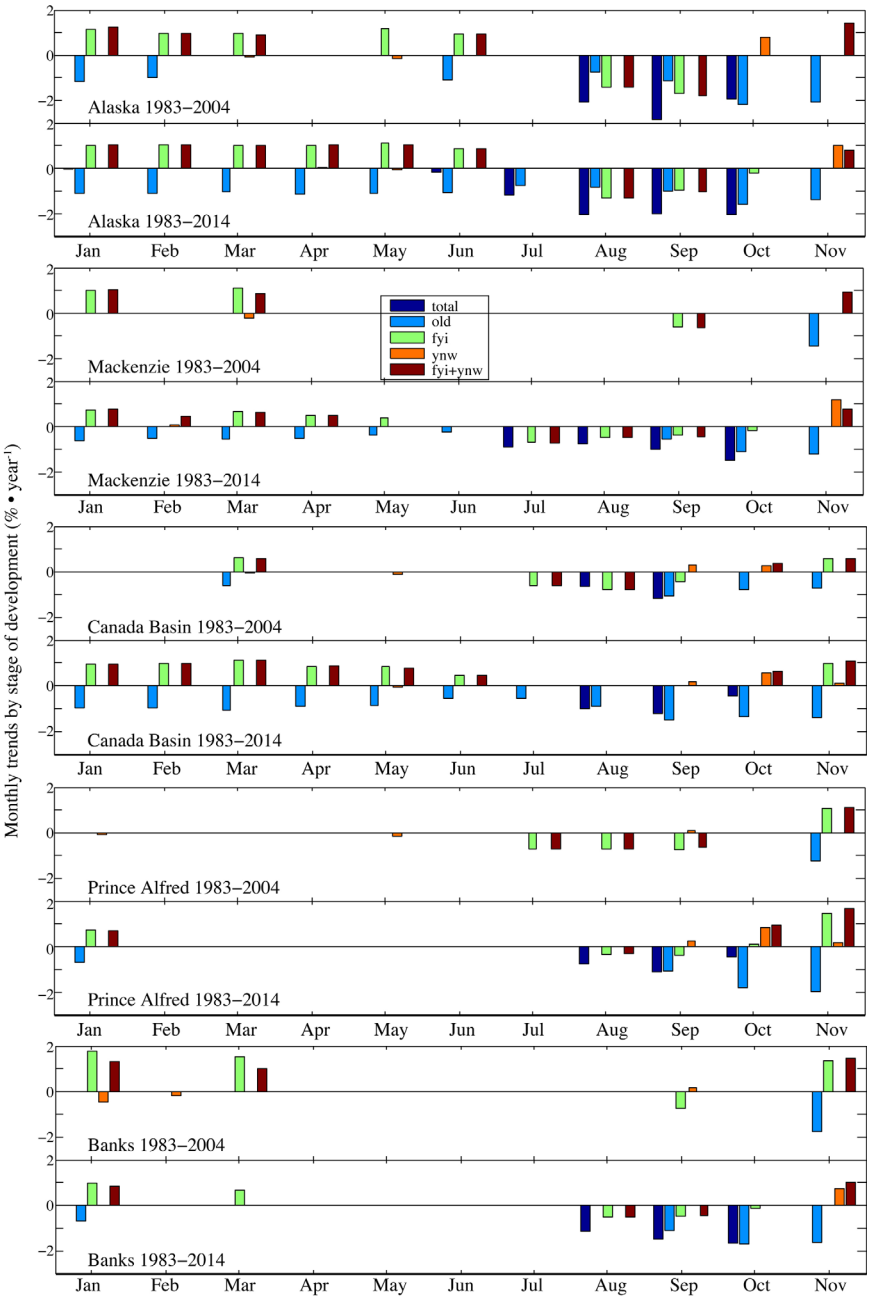

Figure 7. Trends (% yr^{-1}) in monthly mean sea ice concentration by stage of development in the CIS ice regime subregions that make up the Beaufort region from 1983 to 2004 and from 1983 to 2014. Trend data only presented where $p < 0.10$.

same time as the periphery of the mobile pack composed largely of old sea ice in winter (Figure 8). The spatial pattern of open water timing is similar to the start of breakup. The Cape Bathurst flaw lead polynya complex is first to reach break up end, less than two weeks after breakup start on average, indicating that breakup is dynamically forced [e.g., *Steele et al.*, 2015]. Mean breakup in the flaw lead region between 1983 and 2014 is about a week later than it was in the 22 year time series.

Breakup occurs over a larger portion of the region with the addition of the last decade to the time series (Figures 8a, 8b, 8e, and 8f) because the retreat of the summer ice extent has accelerated over that decade. Linear trends over the 1983–2014 time series reveal that breakup start has been getting earlier by about 2 weeks·$decade^{-1}$ in the Alaska subregion; these trends have become more spatially uniform since 2004 (Figures 8c, 8d, 8g, and 8h). Trends toward earlier breakup starts also occurred in the eastern half of the M'Clure

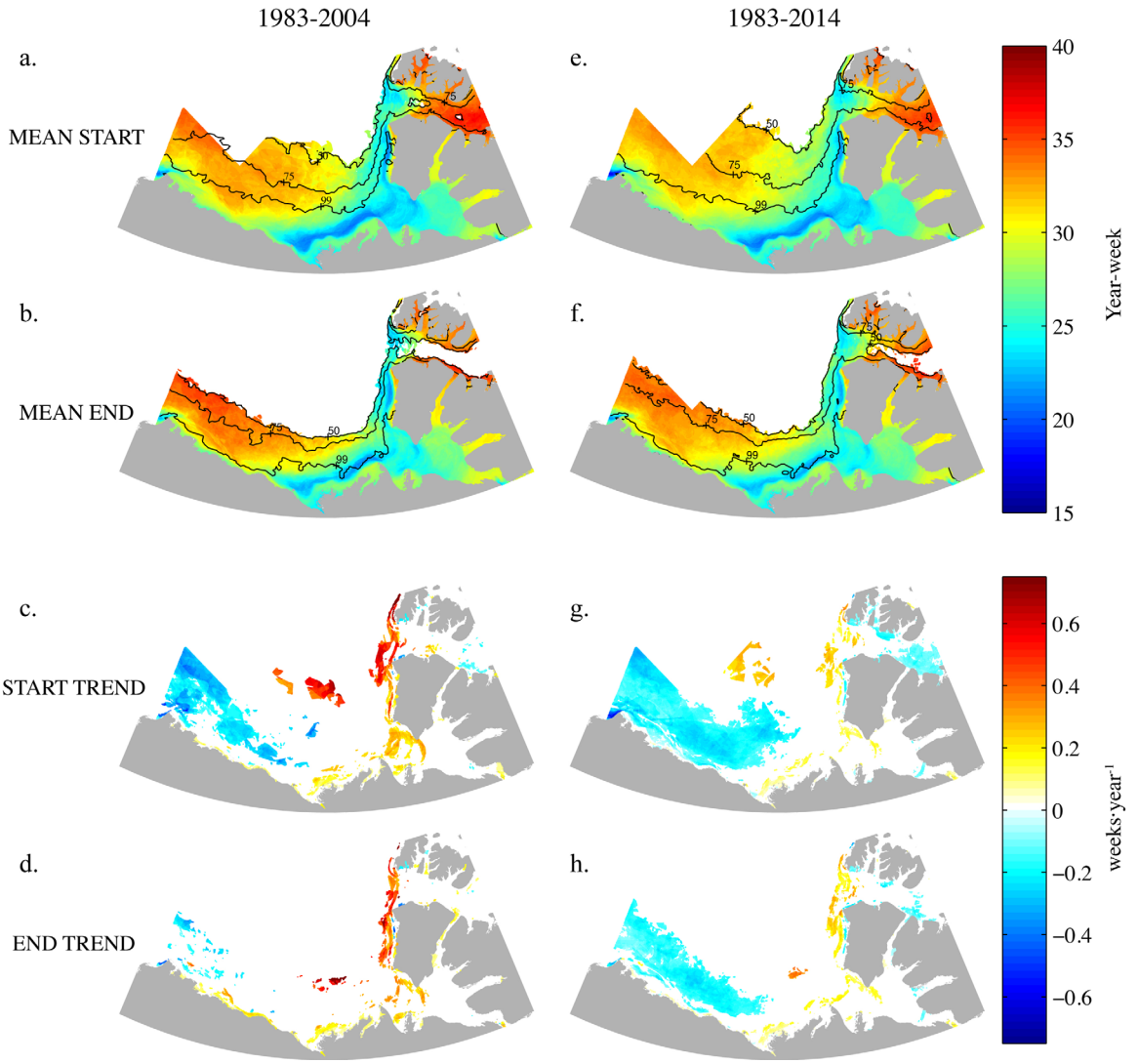

Figure 8. The mean year-week of (a, e) breakup start and (b, f) breakup end for the 1983–2004 and 1983–2014 time series. Trends in the year-week of breakup (c, g) start and (d, h) end through the two time series. Data shown for each grid cell where breakup occurred at least 50% of the years in the time series interrogated. Percent occurrence contours (50%, 75% and 99% from north to south) are overlaid on the mean maps. Trend data only presented where $p < 0.10$.

subregion. Trends toward later breakup start were found in the 32 year time series in the flaw lead polynya region zonally along the Tuktoyaktuk Peninsula, in Amundsen Mouth, and meridionally along the west coast of Banks Island (Figures 8g and 8h).

The percent occurrence of breakup end contours (Figures 8b and 8f) indicate that not all areas that experience break up eventually achieve open water (ice concentration <2/10ths), but the spatial extent of open water is greater in the 1983–2014 time series than in the 1983–2004 time series. In particular, the M'Clure and Alaska subregions stand out with much higher percent occurrence of breakup end in the 32 year period (Figure 8f) reaching breakup end in almost all the years between 2005 and 2014.

The end of break up (start of open water) in the Alaska subregion and the eastern half of the M'Clure subregion has gotten earlier by ~2 weeks·decade^{-1} between 1983 and 2014 (Figure 8h), a marked change from the 1983–2004 time series (Figure 8d). Positive trends indicating later breakup end dates through the 32 year period occurred zonally across the Tuktoyaktuk Peninsula, across the mouth of Amundsen Gulf between Cape Bathurst and Sachs Harbour, and meridionally along the west coast of Banks Island and the western end of the M'Clure subregion (that is, in the flaw lead polynya) (Figure 8h). In M'Clure Strait trends toward later breakup end dates are collocated with substantial reductions total and old sea ice in the

summer and fall months (Figure 6) as well as with reductions in mean old ice concentration and corresponding increases in mean first-year sea ice concentrations in winter (Figure 2). The trends toward later breakup end dates south of M'Clure Strait in the Cape Bathurst flaw lead polynya complex (Figure 8h) are collocated with negative trends in the new-plus-young sea ice concentrations in winter and corresponding positive trends in winter first-year sea ice concentrations (Figures 2d, 2h, 2i, 6, and 7).

Mean breakup end (start of open water) timing is earlier by up to 3 weeks in the Alaska subregion, by 2 weeks in the offshore areas of the Mackenzie subregion, and by about 1 week in the Amundsen subregion between 1983 and 2014 (Figure 8f) compared to 1983–2004 (Figure 8b). Areas within the Cape Bathurst flaw lead polynya complex had mean breakup end dates (1983–2014) that were up to 3 weeks later than the mean breakup end dates for the 22 year period. Farther north in the western half of the M'Clure subregion, the mean breakup end dates for the 32 year period (Figure 8f) are much later than for 1983–2004 (Figure 8b). Very short mean breakup duration calculated for each grid cell in the study area has not changed between 1983–2004 and 1983–2014, again indicating the largely dynamic nature of the ice removal process in the region.

3.5. Sea Ice Freeze Up

The end of open water (freeze up start) occurs earliest in the northern reaches of the study region, specifically in the Prince Alfred subregion (Figure 9), where the mean summer concentrations were highest and composed almost entirely of old sea ice between 1983 and 2014 (Figure 4). The M'Clure subregion is next to experience freeze up start from west to east between year-weeks 35–39 (September). The start of freeze up proceeds west into the Canada basin subregion and southward from the summer old ice pack area in the Prince Alfred subregion into the Mackenzie subregion around year-week 40 ($\sim$ 1 October). Freeze up start then continues zonally west into the Alaska subregion and the east into the Amundsen Mouth and Amundsen subregions in the third and fourth weeks of October (year-weeks 42–43) on average (1983–2014) (Figure 9). Summer ice-free areas of the study region reached freeze up start $\sim$1 week later on average between 1983 and 2014 compared to 1983–2004, except in the Banks subregion where the mean 1983–2014 start of freeze up occurred up to 5 weeks later than in 1983–2004 (Figure 9).

Freeze up start occurrence is higher over more of the region with the addition of 2005–2014 to the time series (see occurrence contours on Figures 9a and 9e), given summer decreases in total ice in the same areas (e.g., Figures 4, 6, and 7). Freeze up is now occurring more often in more of the study region because more of the region is ice-free in summer. Specifically, occurrence of freeze up start in the M'Clure region is increased by the addition of 2005–2014 to the time series (Figures 9g and 9h) linked to the dramatic observed reduction in the summer total and old sea ice concentrations in that subregion (e.g., Figure 6). It follows in the freeze up trends (Figures 9c, 9d, 9g, and 9h, only shown where $p < 0.10$) that the summer mean ice-free areas (Alaska, Mackenzie, Amundsen Mouth, Amundsen, Banks and the east side Prince Alfred) (Figure 4), have experienced significant trends toward later freeze up start date over the period 1983–2014 on the order of 1–2 weeks·decade^{-1} (Figure 9g). When compared to the trends computed for the start of freeze up over the 22 year period (1983–2004), it becomes apparent that although the addition of the years 2005–2014 have not substantially altered the magnitude of the trends toward later freeze up start in the region (save for the M'Clure Strait subregion), the spatial extent of trends toward later freeze up start (end of open water) increased dramatically (Figures 9c and 9g).

The spatial pattern of the timing of freeze up end over the period 1983–2014 is nearly identical to that of freeze up start, and freeze up start and end over the 32 year period (Figures 9b and 9f) are nearly simultaneous in the subregions that experience low sea ice concentrations or ice-free conditions in summer (Figure 4). In the 1983–2014 time series, the freeze up end percent occurrence is higher over a greater portion of the study region than in the 1983–2004 time series, corresponding spatially to reduced summer sea ice concentrations over the 32 year period (Figures 4d–4f and 5). This effect is highlighted in M'Clure Strait, as well as along the transition zone of the summer old ice pack, which moved northward and eastward with the addition of 2005–2014 to the time series (Figures 4d and 4e).

Linear trends in freeze up end timing over the two periods indicate that the addition of 2005–2014 has substantially increased the spatial extent of trends toward later freeze up (Figures 9d and 9h). Between 1983 and 2004, the Alaska subregion contained trends that showed delay in freeze up end by 1–2 weeks·decade^{-1}. With the addition of 2005–2014 to the trend analysis, regions of low total sea ice concentrations or ice-free conditions in summer (namely the Alaska, Mackenzie, Amundsen Mouth, Amundsen subregions) now exhibit

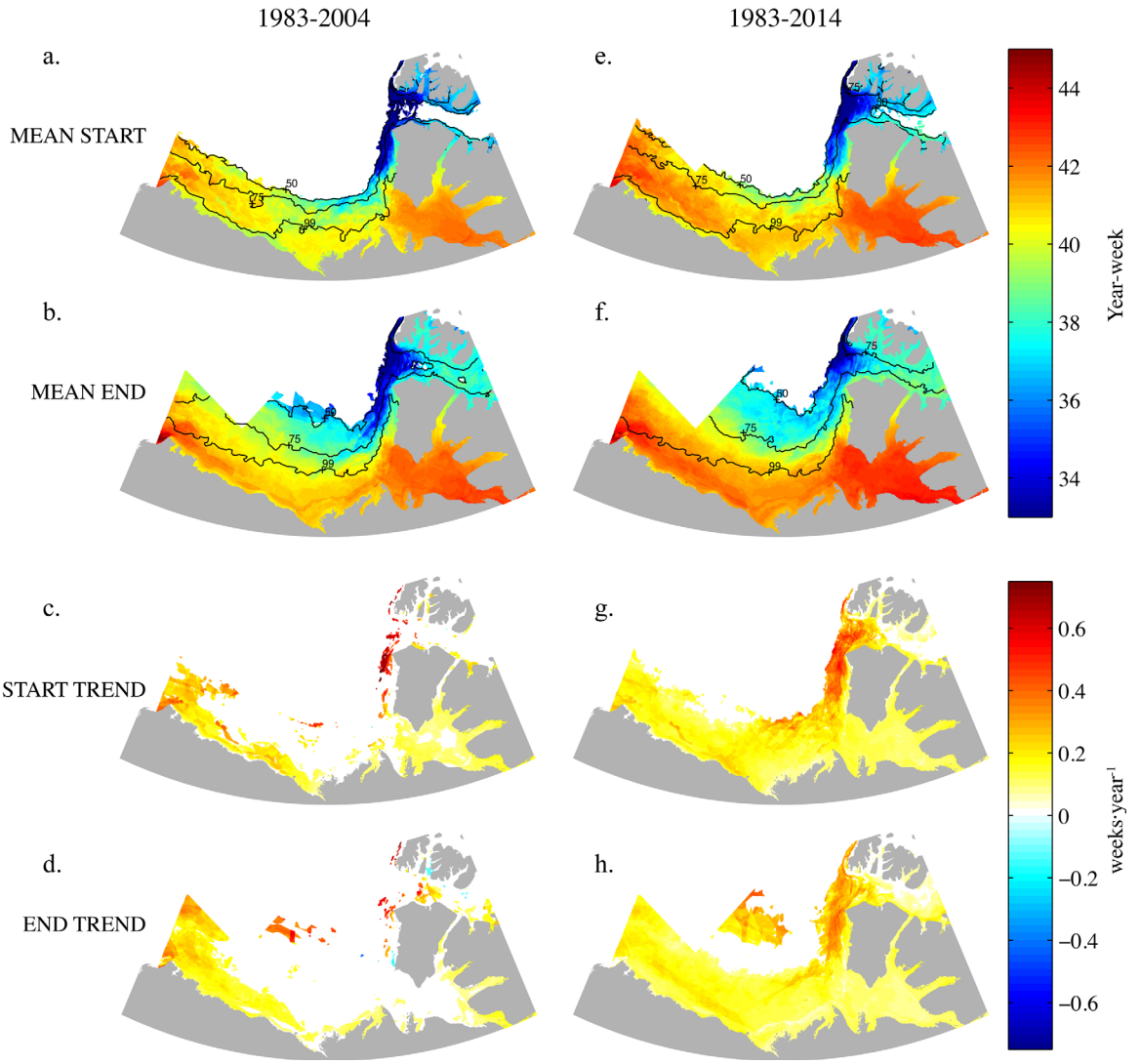

Figure 9. The mean year-week of (a, e) freeze up start and (b, f) freezeup end for the 1983–2004 and 1983–2014 time series. Trends in the year-week of (c, g) freezeup start and (d, h) freeze up end through the two time series. Data shown for each grid cell where freezeup occurred at least 50% of the years in the time series interrogated. Percent occurrence contours for the start and end of freeze up (50%, 75% and 99% from north to south) are overlaid on the mean maps. Trend data only presented where $p < 0.10$.

ubiquitous delays in the end of freeze up by 1–2 weeks·decade^{-1} (Figures 9d and 9h). The M'Clure and Banks subregions show significant ($p < 0.10$) and substantial (up to 3 weeks·decade^{-1}) trends toward later freeze up end dates in the 1983–2014 time series (Figure 9h) spatially coincident with substantial reduction in mean summer old ice (M'Clure: July, August, September, October (Figure 6)) and monthly (Banks: August, September, October, and November (Figure 7)) sea ice concentrations. Freeze up end in the Banks subregion and across the mouth of M'Clure Strait was up to three weeks later in the 32 year period than the 22 year period ending in 2004 (Figure 9h).

3.6. Open Water Season

Open water duration between breakup end and freeze up start is greatest (exceeding 20 weeks) in the Cape Bathurst flaw lead polynya complex, and within the Amundsen Mouth and Amundsen subregions (Figure 10c) where the winter concentration of first-year sea ice makes up the winter total sea ice concentration (Figure 2e). The mean open water season for both periods gets shorter to the north and west as the mean summer (Figure 4) and winter sea ice (Figure 2) concentrations are increasingly composed of old ice reducing the percent occurrence of open water (Figure 10). The west end of the M'Clure subregion exhibits a longer open water season on average than any other area at that latitude. The mean open water duration differences between 1983–2004 and 1983–2014 are spatially highlighted in Figure 11. The areas of the

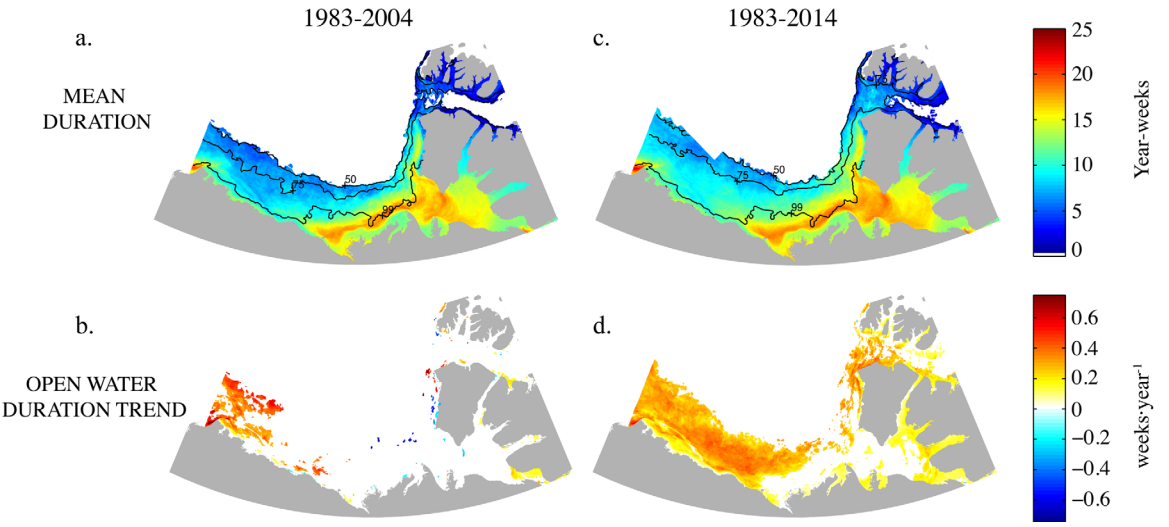

Figure 10. (a, c) Mean open water mean duration and (b, d) trends in the duration of open water between 1983 and 2004 (left column) and 1983–2014 (right column). Percent occurrence contours (50%, 75%, and 99% from north to south) are overlaid on the mean duration maps. Trend data only presented where $p < 0.10$.

study region composed of five tenths first-year sea ice or greater in winter (Figure 2e) have experienced mean open water duration up to three weeks longer in 1983–2014 than in 1983–2004, with the largest difference in open water duration at the transition between the predominately old ice area in Canada basin and Prince Alfred and the predominately first-year sea ice areas in the Alaska, Mackenzie and Banks subregions (Figure 11a). The addition of 2005–2014 to the time series has also lengthened the mean open water season in the Amundsen Mouth and Amundsen subregions. The difference map between the 22 year and 32 year periods in the percent occurrence of open water (Figure 11b) further elucidate marked increase in the occurrence of open water in the old-to-first year sea ice transition zone.

Linear trends in open water duration between the two periods show a substantial increase in the spatial extent of trends toward longer open water seasons annually in the study region; the flaw lead area both along the continental and Banks Island coasts, the entire Alaska and M'Clure subregions, and the coastal margins of the Amundsen subregion all show positive trends of up to three weeks·decade^{-1} in open water duration between 1983 and 2014 (Figure 10d).

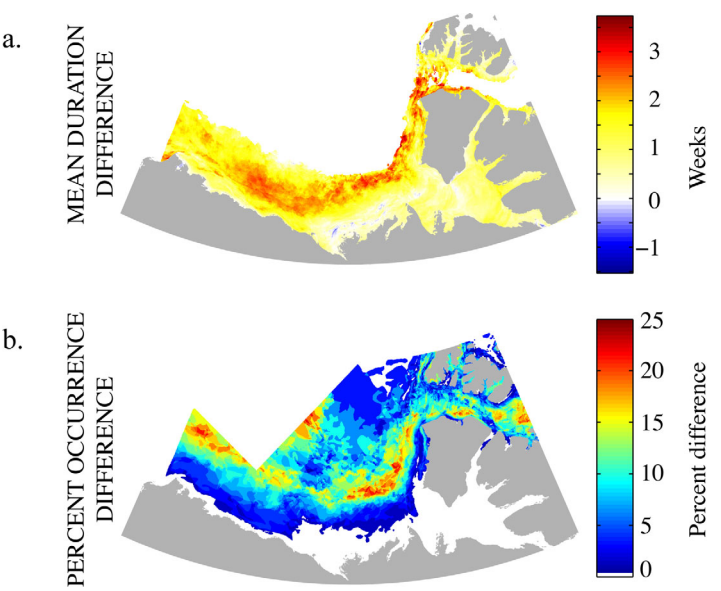

Figure 11. (a) The difference in mean open water duration where positive values represent a longer open water season in the 1983–2014 time series. (b) The difference in percent occurrence of open water between the two periods where positive values indicate greater percent occurrence of open water in the 1983–2014 period. Values are presented in both Figures 11a and 11b in grid cells that experience open water in at least 50% of years.

The addition of the years 2005–2014 to the earlier 1983–2004 time series shows significant and substantial delays in freeze up timing and increased open water season duration in the study area (Figure 12). Results clearly indicate that freeze up timing has experienced large changes compared to very small changes in breakup timing (Figure 12). Delays in freeze up timing have intensified increasing trends in open water duration in almost the entire study region in the 32 year time series (Figure 12).

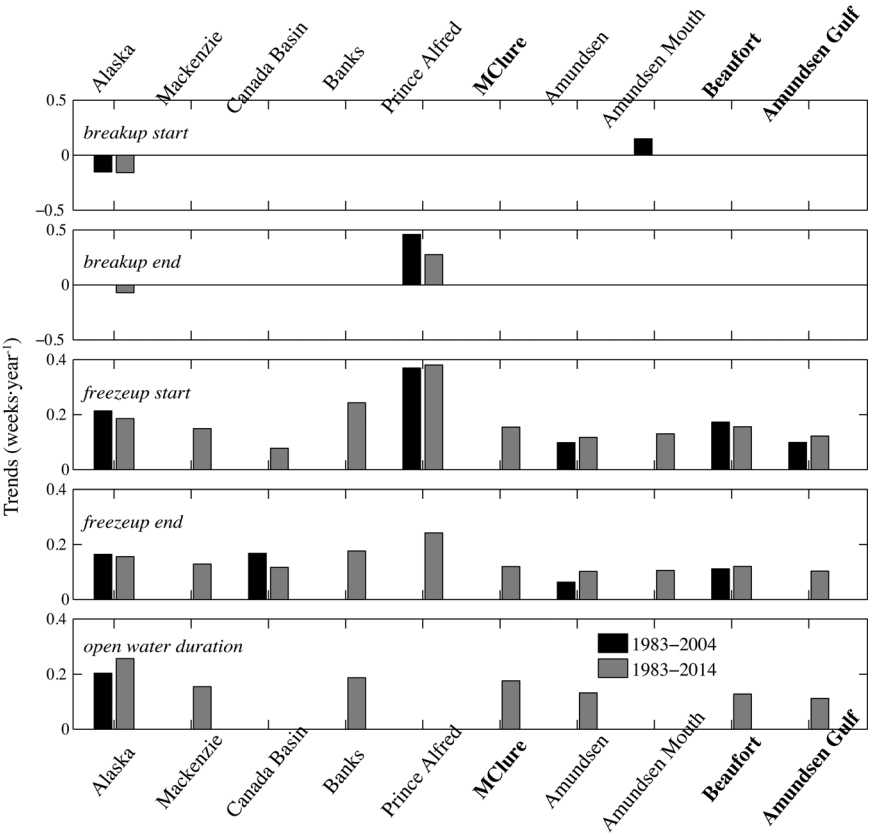

Figure 12. Linear trends (weeks yr^{-1}) in the mean breakup start, breakup end, freeze up start, freeze up end, and open water duration between 1983 and 2004 (black) and 1983–2014 (grey) for each of the (sub) regions specified in figure 1. Positive breakup trends indicate later breakup and positive freeze up trends indicate later freeze up. Positive open water duration indicates longer open water duration. All trends shown only where $p < 0.10$.

4. Discussion

This study highlights a marked shift in the Beaufort ice pack over the last decade, specifically the significant replacement of old ice with first-year sea ice throughout Canada's western Arctic region, and considerable delays in freeze up that increase the length of the open water season. This study corroborates a positive feedback loop in the annual evolution of sea ice concentration by stage of development in Canada's western Arctic. Summer total sea ice concentrations are decreasing more rapidly over larger areas and for a greater number of months each year. Reductions in total sea ice are largely the result of decreasing old sea ice and to a lesser extent decreasing first-year sea ice concentrations in the same months. Reduction in summer sea ice concentrations and extent and lengthening open water duration throughout the study region are followed by observed delay in the thermodynamic freeze up process in autumn. Delayed freeze up is further evidenced by increasing new-plus-young sea ice concentrations later in the autumn; summer old sea ice reductions over much of the study region also propagate through the autumn, winter and spring, with first-year sea ice taking up the slack once the ice cover is complete.

Upon breakup of the winter sea ice cover, more of the region's surface is covered by increasingly thin sea ice (first year ice that formed later than average in the previous autumn and less old ice held over from the previous summers' melt), melting more quickly and completely in summer. Our results indicate that breakup timing is almost completely unchanged in the long term while freeze up timing in the region continues to be annually delayed, increasing annual open water durations. Summer open water at break up end and solar transmission through thinner ice with lower surface albedos as a result of relatively thin end-of-winter sea ice thicknesses are hypothesized to be thermodynamically altering sea ice/ocean surface and delaying freeze up. *Stroeve et al*. [2014] indicate that negative trends in surface albedo from the Advanced Very High Resolution Radiometer (AVHRR) extended Polar Pathfinder (APP-x) in the Beaufort, Chukchi and East Siberian

Seas dominate from May to September between 1982 and 2011. Results also indicate that the absorbed solar radiation anomalies have likely caused increased sea surface temperatures (especially in August and September) that may delay fall freeze up [*Perovich et al*., 2008; *Stroeve et al*., 2014; *Babb et al*., 2016].

In addition, recent summer pressure anomalies have revealed anticyclonic circulation over the Arctic combined with low-pressure anomalies over our study region [*Ogi and Wallace*, 2012]. This anticyclonic circulation has contributed to recent anomalously low sea ice concentrations; results have indicated that anticyclonic circulation anomalies likely induce anomalous Ekman drift of the sea ice toward the central Arctic, which would increase the areal coverage of open water over the marginal seas. So dynamic forcing on sea ice may also contribute to increasing annual open water duration in the Beaufort Sea.

New-plus-young sea ice makes up a small proportion of the total sea ice in the region in autumn and winter, but it represents the regionally and hemispherically significant Cape Bathurst flaw lead polynya complex. It is possible and indeed probable that reductions in summer sea ice coverage in the Beaufort Sea, having shrunk back westward from Banks Island and northward from the ice pack's southern edge, changed the location of the transition zone between the old ice-dominated Beaufort ice pack and its first year sea ice-dominated peripheral coastal areas surrounding the old ice pack and within Amundsen Gulf. Movement of the old to first year transition zone and the resulting increase in the proportion of the region dominated by first-year sea ice is postulated to have affected the physical processes that form and maintain the Cape Bathurst flaw lead polynya complex. Mean winter new-plus-young sea ice concentrations that connote the polynya complex are in decline (Figures 2f and 2i) and trends in the areas occupied by new-plus-young sea ice concentrations in winter (Figure 3h) show increasingly delayed breakup in these areas since 1983 (Figure 8), potentially signaling changes in flaw lead polynyas annual operation.

Massive observed replacement of old ice by first year ice in M'Clure Strait throughout the annual cycle in the 1983–2014 time series did not occur in the 1983–2004 time series (Figure 6). Changes in the old-to-first year sea ice transition zone likely contribute to the massive changes witnessed in M'Clure Strait sea ice in the 32 year time series. We hypothesize that the receding of the Beaufort Sea old ice pack westward from the mouth of M'Clure Strait (Figures 2 and 4) throughout the annual cycle has made the annual evolution of M'Clure Strait at present (Figure 6) very similar to the average historical evolution of Amundsen Gulf, which has been dominated by first-year sea ice at the end of winter and linked to the off-shelf Beaufort old sea ice pack through the old-to-first year transition zone for the past 32 years (Figure 2).

Decreased summer old sea ice concentrations in M'Clure, Canada basin and Alaska have created higher percent occurrence of freeze up start in those subregions––a greater portion of the entire study area is now freezing up thermodynamically in the fall rather than being filled dynamically with old sea ice from the north [e.g., *Maslanik et al*., 2011]. Fall freeze up occurred up to 5 weeks later in the Banks subregion on average between 1983 and 2014 compared to 1983–2004, indicating a shift toward thermodynamic freeze up west of Banks Island since 2004 as a result of long-term losses of sea ice in the region both on average in summer, and monthly average losses during July, August, September, and November for the 32 year period.

The freeze up duration (the time between freeze up start and end) of up to 5 weeks in the Banks and M'Clure (sub)regions in the 1983–2004 time series was reduced to 3 weeks in the 1983–2014 time series; It follows that the start of freeze up should be regarded as the primary indicator of freeze up in the seasonal sea ice areas because the main hindrance to freeze up in these areas is the export of heat to the atmosphere from the open ocean surface after it has warmed all summer. The presence of 2/10ths sea ice concentration indicates that the ocean surface is likely at the freezing temperature, having lost its heat accumulated over the summer. Two-tenths ice concentration further likely acts to seed sea ice growth spatially, which allows the achievement of 8/10ths sea ice concentration with little delay.

5. Conclusions

The annual evolution of sea ice by stage-of-development in the study region changed dramatically from 1983 to 2014, and the changes observed were larger in magnitude with the addition of the last decade (2005–2014) to the time series analyzed here. Between 1983 and 2014, summer reductions in total sea ice concentration between −10% and −15%·decade^{-1} via reductions in old (−5% to −10%·decade^{-1}) and first-year sea ice (−5%·decade^{-1}) concentrations over increasingly large areas and in more months per

year. Total sea ice losses were observed to occur earlier in summer (e.g., June and July) in the southerly and westerly parts of the study region in the 1983–2014 time series compared to the time series ending in 2004. Those summer changes are followed by thermodynamic freeze up that became increasingly delayed and occurred over an increasingly large area through the 32 year period (1983–2014) interrogated. Delay in thermodynamic freeze up and dynamic forcing on the sea ice has increased the summer open water duration in much of the study region. Although no temporal or spatial change occurred in the complete total sea ice cover throughout the study area upon the end of freeze up, autumnal sea ice cover was decreasingly composed of old ice, and increasingly composed of new-plus-young sea ice. This is followed by a similarly complete winter and spring sea ice cover that was increasingly composed of first year ice at the expense of old ice concentrations at a rate up to 15% decade^{-1} from January to breakup. Breakup timing has not significantly changed in most of the study region, with the caveat that break up is now occurring later in the Alaska subregion and earlier in the Prince Alfred subregion. Further work will focus on regional and subregional thermodynamic and dynamic forcing of the trends observed here. It may also include a comparison study with the NSIDC sea ice age product [*Tschudi et al.*, 2015].

Acknowledgments

Thanks to the Canadian Ice Service for providing the digitally archived chart data online. These unrestricted data are available at: http://iceweb1.cis.ec.gc.ca/Archive/page1.xhtml;jsessionid= F7AF5BF1DA6865EC213D8E224F48FB97? lang=en. The Canada Excellence Research Chair program (SR), the Canada Research Chair program (DGB), and the Natural Sciences and Engineering Research Council of Canada (RJG) contributed funding to this study. This work is a contribution to the Arctic Science Partnership (asp-net.org) and the ArcticNet Networks of Centres of Excellence program.

References

Agnew, T. A., and S. Howell (2003), The use of operational ice charts for evaluating passive microwave ice concentration data, *Atmos. Ocean*, *41*(4), 317–331, doi:10.3137/ao.410405.

Arrigo, K., and G. van Dijken (2004), Annual cycles of sea ice and phytoplankton in Cape Bathurst polynya, southeastern Beaufort Sea, Canadian Arctic, *Geophys. Res. Lett.*, *31*, L08304, doi:10.1029/2003GL018978.

Babb, D., R. J. Galley, D. G. Barber, and S. Rysgaard (2016), Physical processes contributing to an ice free Beaufort Sea during September 2012, *J. Geophys. Res. Oceans*, *121*, 267–283, doi:10.1002/2015JC010756.

Barber, D. G., and J. M. Hanesiak (2004), Meteorological forcing of sea ice concentrations in the southern Beaufort Sea over the period 1979 to 2000, *J. Geophys. Res.*, *109*, C06014, doi:10.1029/2003JC002027.

Barber, D. G., and R. A. Massom (2007), The role of sea ice in Arctic and Antarctic polynyas, in *Polynyas: Windows to the World*, edited by W. O Smith and D. G. Barber, *Elsevier Oceanogr. Ser.*, 74, 1–54, doi:10.1016/S0422-9894(06)74002-8.

Carmack, E. C., and R. W. Macdonald (2002), Oceanography of the Canadian Shelf of the Beaufort Sea: A setting for marine life, *Arctic*, *55*, suppl. 1, 29–45.

Cavalieri, D. J., C. L. Parkinson, P. Gloersen and H. Zwally (1996), *Sea Ice Concentrations From Nimbus-7 SMMr and SMSP SSM/I-SSMIS Passive Microwave Data*, NASA Natl. Snow and Ice Data Cent. Distrib. Active Arch. Cent., Boulder, Colo., doi:10.5067/8GQ8LZQVLOVL.

CIS (2007), Canadian Ice Service Digital Archive––Regional Charts: Canadian Ice Service ice regime regions (CISIRR) and sub-regions with associated data quality indices, *CIS Arch. Doc. Ser.*, *3*, pp. 1–63. [Available at http://ice.ec.gc.ca/IA_DOC/cisads_no_003_e.pdf.]

Comiso, J. C. (2012), Large decadal decline of the Arctic multiyear ice cover, *J. Clim.*, *25*, 176–1193, doi:10.1175/JCLI-D-11-00113.1.

Deser, C., and H. Teng (2008), Evolution of Arctic sea ice concentration trend and the role of atmospheric circulation forcing, 1979-2007, *Geophys. Res. Lett.*, *35*, L02504, doi:10.1029/2007GL032023.

Else, B. G. T., T. Papakyriakou, R. J. Galley, A. Mucci, M. Gosselin, L. Miller, E. Shadwick, and H. Thomas (2012), Annual cycles of pCO_{2sw} in the Southeastern Beaufort Sea: New understandings of air-sea CO_2 exchange in Arctic polynya regions, *J. Geophys. Res.*, *117*, C00G13, doi:10.1029/2011JC007346.

Fequet, D. (Ed.) (2005), *Manual of Standard Procedures for Observing and Reporting Ice Conditions*, 9th ed., Can. Ice Serv., Environ. Canada, Ottawa.

Fetterer, F., K. Knowles, W. Meier, and M. Savoie (2002), *Sea Ice Index, Version 1*, Natl. Snow and Ice Data Cent., Boulder, Colo., doi:10.7265/N5QJ7F7W.

Galley, R. J., E. Key, D. G. Barber, B. J. Hwang, and J. K. Ehn (2008), Spatial and temporal variability of sea ice in the southern Beaufort Sea and Amundsen Gulf: 1980-2004, *J. Geophys. Res.*, *113*, C05S95, doi:10.1029/2007JC004553.

Galley, R. J., B. G. T. Else, S. E. L. Howell, J. V. Lukovich, and D. G. Barber (2012), Landfast sea ice conditions in the Canadian Arctic, *Arctic*, *65*(2), 133–144.

Galley, R. J., B. G. T. Else, S. J. Prinsenberg, D. Babb and D. G. Barber (2013), Summer sea ice concentration, motion and thickness near areas of proposed offshore oil and gas development in the Canadian Beaufort Sea–2009, *Arctic*, *66*(1), 105–116.

Haas, C. (2004), Late-summer sea ice thickness variability in the Arctic Transpolar Drift 1991-2001 derived from ground-basedelectromagnetic sounding, *Geophys. Res. Lett.*, *31*, L09402, doi:10.1029/2003GL019394.

Haas, C., S. Hendricks, H. Eicken, and A. Herber (2010), Synoptic airborne thickness surveys reveal state of Arctic sea ice cover, *Geophys. Res. Lett.*, *37*, L09501, doi:10.1029/2010GL042652.

Hammill, M. O. (1987), The effects of weather on ice conditions in the Amundsen Gulf, N.W.T., *Rep. 1900*, 10 pp., Dep. of Fish. and Oceans Can., Ste-Anne-de-Bellevue, Quebec, Canada.

Hansen, E., S. Gerland, M. A. Granskog, O. Pavlova, A. H. H. Renner, J. Haapala, T. B. Løyning, and M. Tschudi (2013), Thinning of Arctic sea ice observed in Fram Strait: 1990–2011, *J. Geophys. Res. Oceans*, *118*, 1–20, doi:10.1002/jgrc.20393.

Hutchings, J. K., and I. G. Rigor (2012), Role of ice dynamics in anomalous ice conditions in the Beaufort Sea in 2006, and 2007, *J. Geophys. Res.*, *117*, C00E04, doi:10.1029/2011JC007182.

Kwok, R., and G. F. Cunningham (2010), Contribution of melt in the Beaufort Sea to the decline in Arctic multiyear sea ice coverage: 1993–2009, *Geophys. Res. Lett.*, *37*, L20501, doi:10.1029/2010GL044678.

Kwok, R., and D. A. Rothrock (2009), Decline in Arctic sea ice thickness from submarine and ICESat records: 1958–2008, *Geophys. Res. Lett.*, *36*, L15501, doi:10.1029/2009GL039035.

Kwok, R., G. F. Cunningham, M. Wensnahan, I. Rigor, H. J. Zwally, and D. Yi (2009), Thinning and volume loss of the Arctic sea ice cover: 2003-2008, *J. Geophys. Res.*, *114*, C07005, doi:10.1029/2009JC005312.

Maslanik, J., J. Stroeve, C. Fowler, and W. Emery (2011), Distribution and trends in Arctic sea ice age through spring 2011, *Geophys. Res. Lett.*, *38*, L13502, doi:10.1029/2011GL047735.

Maslanik, J. A., C. Fowler, J. Stroeve, S. Drobot, J. Zwally, D. Yi, and W. Emery (2007), A younger, thinner Arctic ice cover: Increased potential for rapid extensive sea-ice loss, *Geophys. Res. Lett.*, *34*, L24501, doi:10.1029/2007GL032043.

Moore, D. S. (1995), *The basic practise of statistics*, W. H. Freeman and Company, N. Y.

National Ice Center (2009), *National Ice Center Arctic Sea Ice Charts and Climatologies in Gridded Format, Version 1*, compiled by F. Fetterer and C. Fowler, Natl. Snow and Ice Data Cent., Boulder, Colo., doi:10.7265/N5X34VDB.

Ngheim, S. V., Y. Chao, G. Neumann, P. Li, D. K. Perovich, T. Street, and P. Clemente-Colòn (2006), Depletion of perennial sea ice in the East Arctic Ocean, *Geophys. Res. Lett.*, *33*, L17501, doi:10.1029/2006GL027198.

Ogi, M., and I. Rigor (2013), Trends in Arctic sea ice and the role of atmospheric circulation, *Atmos. Sci. Lett.*, *14*, 97–101, doi:10.1002/asl2.423.

Ogi, M., and J. M. Wallace (2012), The role of summer surface wind anomalies in the summer Arctic sea ice extent in 2010 and 2011, *Geophys. Res. Lett.*, *39*, L09704, doi:10.1029/2012GL051330.

Ogi, M., and K. Yamazaki (2010), Trends in the summer Northern Annular Mode and Arctic sea ice, *SOLA*, *6*, 041–044, doi:10.2151/sola.2010-011.

Parkinson, C. L. (2014), Spatially mapped reductions in the length of the Arctic sea ice season, *Geophys. Res. Lett.*, *41*, 4316–4322, doi:10.1002/2014GL060434.

Perovich, D. K., J. A. Richter-Menge, K. F. Jones, and B. Light (2008), Sunlight, water and ice: Extreme Arctic sea ice melt during the summer of 2007, *Geophys. Res. Lett.*, *35*, L11501, doi:10.1029/2008GL034007.

Perovich, D. K., J. A. Richter-Menge, K. F. Jones, B. Light, B. C. Elder, C. Polashenski, D. Laroche, T. Markus, and R. Lindsay (2011), Arctic sea-ice melt in 2008 and the role of solar heating, *Ann. Glaciol.*, *52*(57), 355–359.

Steele, M., S. Dickinson, J. Zhang, and R. W. Lindsay (2015), Seasonal ice loss in the Beaufort Sea: Toward synchrony and prediction, *J. Geophys. Res. Oceans*, *120*, 1118–1132, doi:10.1002/2014JC010247.

Stroeve, J., M. Serreze, S. Drobot, S. Gearhead, M. Holland, J. Maslanik, W. Meier, and T. Scambos (2008), Arctic sea ice extent plummets in 2007, *Eos Trans. AGU*, *89*(2), 13, doi:10.1029/2008EO020001.

Stroeve, J. C., T. Markus, L. Boisvert, J. Miller, and A. Barrett (2014), Changes in Arctic melt season and implications for sea ice loss, *Geophys. Res. Lett.*, *41*, 1216–1225, doi:10.1002/2013GL058951.

Tivy, A., S. E. L. Howell, B. Alt, S. McCourt, R. Chagnon, G. Crocker, T. Carrieres, and J. J. Yackel (2011), Trends and variability in summer sea ice cover in the Canadian Arctic based on the Canadian Ice Service digital archive, 1960-2008 and 1968-2008, *J. Geophys. Res.*, *116*, C03007, doi:10.1029/2009JC005855.

Tschudi, M., C. Fowler, and J. Maslanik (2015), *EASE-Grid Sea Ice Age, Version 2*, NASA Natl. Snow and Ice Data Cent. Distrib. Active Arch. Cent., Boulder, Colo., doi:10.5067/1UQJWCYPVX61.

Zhang, J., R. Lindsay, A. Schweiger, and I. Rigor (2012), Recent changes in the dynamic properties of declining sea ice: A model study, *Geophys. Res. Lett.*, *39*, L20503, doi:10.1029/2012GL053545.